The Fas System Confers Protection against Alveolar Disruption in Hyperoxia-Exposed Newborn Mice

Quanfu Mao[1,3], Sravanthi Gundavarapu[1], Chintan Patel[1], Amy Tsai[1], Francois I. Luks[2,4,5], and Monique E. De Paepe[1,3]

[1]Department of Pathology, Women and Infants Hospital, Providence, Rhode Island; [2]Division of Pediatric Surgery, Rhode Island Hospital, Providence, Rhode Island; and Departments of [3]Pathology and Laboratory Medicine, [4]Pediatrics, and [5]Surgery, The Warren Alpert Medical School of Brown University, Providence, Rhode Island

The functional significance of the Fas/Fas-ligand (FasL) system in hyperoxia-induced lung injury and alveolar disruption in newborn lungs *in vivo* remains undetermined. To assess the role of the Fas/FasL system, we compared the effects of hyperoxia (95% O_2 from birth to Postnatal Day [P]7) in Fas-deficient *lpr* mice and wild-type mice. Alveolar disruption was more severe in hyperoxic *lpr* mice than in wild-type mice. In addition, a transient alveolarization defect was noted in normoxic *lpr* mice. Hyperoxia induced marked up-regulation of pulmonary Fas expression in wild-type mice, as well as elevated mRNA levels of pro-apoptotic Bax, Bad, and Bak. Pulmonary apoptotic activity was similar in hyperoxic wild-type and *lpr* mice. In contrast, lung growth and proliferation, assessed by stereologic volumetry and Ki67 proliferation studies, were significantly higher in hyperoxic wild-type mice compared with *lpr* mice, suggesting the Fas/FasL system has a pro-proliferative role in hyperoxic conditions. Levels of the prosurvival MAPkinase, pERK1/2, were significantly higher in hyperoxic wild-type mice compared with *lpr* mice, while pAkt levels were similar. These data suggest that the primary role of the Fas/FasL system in hyperoxic newborn lungs is pro-proliferative, rather than pro-apoptotic, and likely mediated through a Fas-ERK1/2 pathway. Fas-induced proliferation and lung growth in hyperoxic newborn lungs may counteract, in part, the detrimental effects of apoptosis mediated by non-Fas pathways, such as pro-apoptotic Bax/Bcl-2 family members. The capacity of the Fas/FasL signaling pathway to mediate protective rather than destructive functions in hyperoxic newborn lungs highlights the versatility of this complex pathway.

Keywords: CD95; oxygen toxicity; apoptosis; programmed cell death; bronchopulmonary dysplasia

The treatment of advanced respiratory failure often requires supraphysiologic oxygen concentrations to maintain oxygen delivery to peripheral tissues. This condition of hyperoxia may, paradoxically, exacerbate lung damage. Oxygen toxicity has been implicated in the pathogenesis of bronchopulmonary dysplasia (BPD), a chronic lung disease of newborn infants associated with significant mortality and morbidity (1–3). The main pathologic hallmark of post-surfactant BPD is an arrest of alveolar development, characterized by large and simplified distal lung acini that show little evidence of vascularized ridges ("secondary crests") or alveolar septa. Impairment of alveolar formation in BPD leads to long-term global reduction in alveolar number and gas-exchange surface area (4, 5). In addition, lungs of infants with BPD show variable degrees of interstitial fibrosis and structurally abnormal microvasculature (6, 7).

CLINICAL RELEVANCE

This study suggests that the main function of the Fas/FasL signaling system in hyperoxic lungs is pro-proliferative, rather than pro-apoptotic. These data may prompt reappraisal of the functions of the Fas system in the lung.

The pathologic changes in hyperoxic lungs are characterized by injury and death of the alveolar epithelial and endothelial cells (8). Hyperoxia-induced pulmonary cell death may involve necrosis and apoptosis, two distinct mechanisms of cell death that have specific biochemical, morphologic, and functional characteristics (9). In necrosis, acute, nonphysiologic injury leads to extensive cell lysis and disruption of the cell membrane. In contrast, apoptosis represents a regulated form of cell death that typically involves the activation of proteases and nucleases within an intact plasma membrane. Apoptosis has been described as a major death mechanism in hyperoxia-induced lung injury in various animal models *in vivo* (10–13). We have recently investigated the mechanisms and regulation of hyperoxia-induced death in lung epithelial cells *in vitro* (14). We determined that exposure of murine lung epithelial cells (MLE-12 cells) (15) to hyperoxia (95% O_2) induced time-specific sequential patterns of cell death. Caspase-mediated apoptosis was the first morphologically and biochemically recognizable mode of cell death, occurring within 24 to 48 hours of oxygen exposure. This initial wave of apoptosis was followed by necrosis of residual adherent cells that became evident after 72 hours of oxygen exposure.

The effector pathways regulating alveolar epithelial apoptosis in hyperoxia-exposed postcanalicular lungs remain incompletely defined. Cells can undergo apoptosis through two distinct pathways (16). Mitochondrial-dependent apoptosis is primarily regulated by the Bcl-2 protein family. This multimember family can be divided into pro-apoptotic (e.g., Bax, Bad, Bak) and anti-apoptotic (e.g., Bcl-2, Bcl-$_{XL}$) proteins. The activity of Bcl-2 family members is regulated, in part, by dimerization among the various family members (17). The second pathway (receptor-mediated apoptosis [18–20]) involves triggering cell surface "death receptors," a specialized subset of the tumor necrosis factor receptor (TNF-R) superfamily (18–20). The Fas/Fas-ligand (FasL) pathway is the best-studied receptor-mediated death signaling pathway. Stimulation of the receptor Fas (CD95/APO1) by its natural ligand, FasL, or Fas-activating antibody results in recruitment of two key signaling proteins, the adapter protein FADD (Fas-associated death domain, also called MORT-1) and the initiator cysteine protease caspase-8, which together form the death-inducing signaling complex (DISC). Proteolytic autoactivation of DISC results in activation of the effector caspases, including the key effector caspase, caspase-3. Activated caspase-3 cleaves DNA repair enzymes, cellular and nuclear structural proteins, endonu-

(*Received in original form January 28, 2008 and in final form May 23, 2008*)

This work was supported in part by NIH P20-RR18728 (to M.E.D.P.).

Correspondence and requests for reprints should be addressed to Monique E. De Paepe, M.D., Women and Infants Hospital, Dept. of Pathology, 101 Dudley Street, Providence, RI 02905. E-mail: mdepaepe@wihri.org

Am J Respir Cell Mol Biol Vol 39. pp 717–729, 2008
Originally Published in Press as DOI: 10.1165/rcmb.2008-0052OC on June 27, 2008
Internet address: www.atsjournals.org

cleases, and many other cellular constituents, culminating in effective cell death (18–20).

The Fas/FasL death signaling system has been implicated in alveolar type II cell apoptosis in various clinical and experimental models of adult lung injury (21–26). Our recent studies implicated the Fas/FasL death signaling system as important regulator of hyperoxia-induced apoptosis in lung epithelial cells (14). We determined that exposure of MLE-12 cells to hyperoxia induced a 3-fold up-regulation of Fas mRNA and protein expression, synchronous with the apoptotic stage of cell death. Fas gene silencing by RNA interference significantly reduced hyperoxia-induced apoptosis, confirming the critical role of the Fas/FasL system in hyperoxia-induced lung epithelial cell apoptosis *in vitro*.

The role of Fas/FasL in hyperoxia-induced alveolar epithelial apoptosis and alveolar disruption *in vivo* remains unclear. Increased pulmonary Fas mRNA expression has been reported in adult mice exposed to greater than 95% O_2 (27), replicating the *in vitro* effects of hyperoxia. However, the impact of Fas deficiency in hyperoxic adult animals seems controversial. Whereas one study described a lack of protection against hyperoxia-induced lung injury and death in adult Fas-deficient *lpr* mice (27), others reported that Fas deficiency confers partial resistance to hyperoxia-induced apoptosis and death in adult mice with *Legionella* infection (28).

It is uncertain whether data derived from studies in adult mice can be extrapolated to newborn mice, since the systemic and pulmonary responses to hyperoxia are strikingly different in adult and newborn mice. In adult mice, hyperoxia exposure (> 95% O_2) is uniformly lethal within 48 to 72 hours, whereas newborn mice can survive for prolonged periods (> 7 d) under the same conditions. In adult mice, hyperoxia induces extensive acute lung injury, characterized by epithelial and endothelial cell death, acute inflammatory infiltrates, and lung edema. In contrast, the hallmark of hyperoxia in newborn mice is disrupted alveolar development, associated with a more modest inflammatory response. The differences in pulmonary response to hyperoxia in adult and newborn animals suggest that the effects of hyperoxia on pulmonary apoptosis and apoptosis-related gene expression may be age-specific as well. Similarly, striking developmental differences have been described in the response of adult and newborn IL-6 and IL-13 transgenic mice exposed to hyperoxia (29).

In this study, we determined the functional role of Fas/FasL signaling in hyperoxia-induced apoptosis and dysregulated alveolar remodeling in postcanalicular lungs. To this end, apoptosis, apoptosis-related gene expression, and alveolarization of newborn wild-type mice exposed to hyperoxic conditions were compared with those in newborn *lpr* mice, deficient for the Fas receptor. Our results demonstrate that the Fas/FasL signaling system, traditionally associated with cell death, in fact has a protective role in newborn lungs exposed to hyperoxia, and highlight the nonapoptotic functions of this versatile signaling pathway.

MATERIALS AND METHODS

Animals and Tissue Processing

Breeding colonies were established from homozygous matings of inbred C57BL/6J wild-type mice (Jackson Laboratories, Bar Harbor, ME) or Fas-deficient *lpr* mice bred onto the same genetic background (B6.MRL-*Fas*^{lpr}; Jackson Laboratories). The gene mutation in the *lpr* (lymphoproliferation) mouse strain causes defective expression of Fas due to insertion of a transposable element into intron 2 (30). Newborn C57BL/6J mice and *lpr* mice were exposed to room air or hyperoxia (> 95% O_2) for 7 days, starting at birth. For hyperoxia experiments, mice were placed in an airtight plexiglass chamber. Oxygen concentrations were continuously monitored and controlled with an in-line oxygen analyzer and controller system (ProOx 110; BioSpherix, Redfield, NY). Nursing dams were rotated daily between air- and oxygen-exposed litters to minimize maternal oxygen toxicity. Newborn mice were killed by pentobarbital overdose at Postnatal Day (P)7 (P1 = day of birth), corresponding to mid-alveolarization stage (31). Body and wet lung weights were recorded. For molecular analyses, lungs were snap-frozen in liquid nitrogen and stored at −80°C. All animal experiments were conducted in accordance with institutional guidelines for the care and use of laboratory animals.

Analysis of Lung Growth

In lungs processed for molecular analyses, lung growth was assessed by wet lung weight and wet lung weight/body weight ratio. For morphologic and morphometric studies, lungs were formalin-fixed by standardized tracheal instillation *in situ* and lung growth was estimated by determination of inflated lung volume and lung volume/body weight ratio.

Morphometric assessment of growth of peripheral air-exchanging lung parenchyma and contribution of the various lung compartments (airspace versus parenchyma) to the total lung volume was performed using standard stereological volumetric techniques, as previously described (32, 33). The inflated lung volume, V(lu), was determined according to the Archimedes principle (34). The areal density of air-exchanging parenchyma, A_A(ae/lu), was determined by point-counting based on computer-assisted image analysis. The number of points falling on air-exchanging parenchyma (peripheral lung parenchyma excluding airspace) in random lung fields was divided by the number of points falling on the entire field (tissue and airspace). A_A(ae/lu) represents the tissue fraction of the lung and as such is the complement of the airspace fraction A_A(air/lu). The total volume of air-exchanging parenchyma, V(ae), was calculated by multiplying A_A(ae/lu) by V(lu).

Analysis of Alveolarization

For morphologic and morphometric studies, the lungs were formalin-fixed by standardized tracheal instillation at a constant pressure of 20 cm H_2O. All samples were equally inflated and fixed on the same apparatus. The lungs were dehydrated in graded ethanol solutions and embedded in paraffin. Sections (4 μm thick) were stained with hematoxylin and eosin.

Alveolarization was quantified by computer-assisted morphometric analysis of the mean cord length (MCL) and radial alveolar count (RAC). MCLs were determined by superimposing randomly oriented parallel arrays of lines across randomly selected microscope fields of air-exchanging lung parenchyma (at least 25 random fields per lung) and determining the distance between airspace walls (including alveoli, alveolar sacs, and ducts). The RAC was determined by counting the number of septa intersected by a perpendicular line drawn from the center of a respiratory bronchiole to the edge of the acinus (connective tissue septum or pleura), based on analysis of at least 10 randomly selected lung fields.

Analysis of Surfactant System

To determine alveolar type II cell density, sections were immunostained using an antibody against pro–surfactant protein-C (pro–SP-C) (Abcam Inc., Cambridge, MA). Immunoreactivity was detected by streptavidin–biotin immunoperoxidase method followed by 3,3′-diaminobenzidine tetrachloride (DAB). Specificity of staining was demonstrated by omission of primary antibody, which abolished all reactivity. The number of SP-C–immunoreactive type II cells per ×40 high-power field (type II cell density) was determined in 10 randomly selected microscope fields. Pulmonary SP-C levels were determined by Western blot analysis of whole lung lysates.

Analysis of Microvascular Development

For morphometric analysis of vessel density, sections were immunostained for the presence of Factor VIII (von Willebrand factor [vWF]) (DAKO, Carpinteria, CA), an endothelium-specific marker. The number of Factor VIII–positive vessels (20–80 μm in diameter) per high-power field (×20 objective) was counted in 25 randomly selected fields to assess the vessel density. All morphometric assessments were made on coded slides from at least eight animals per group by a single observer who was unaware of the genotype or experimental condition

TABLE 1. BIOMETRY AND LUNG MORPHOMETRY

	Normoxia		Hyperoxia	
	WT	LPR	WT	LPR
Body wt, g	3.52 ± 0.09 (39)	3.25 ± 0.08 (42)*	2.36 ± 0.18 (27)†	2.53 ± 0.09 (62)†
Lung wt (wet), mg	61 ± 2 (26)	57 ± 2 (23)	48 ± 2 (21)†	42 ± 1 (44)†‡
Lung wt (wet)/BW, %	1.78 ± 0.03 (26)	1.78 ± 0.04 (23)	2.11 ± 0.16 (21)	1.77 ± 0.07 (44)‡
V(lung), μl	119 ± 4 (10)	127 ± 4 (15)	99 ± 4 (6)†	116 ± 5 (15)†‡
V(lung)/BW, μl/g	34.5 ± 2.0 (10)	40.2 ± 1.7 (15)*	59.7 ± 4.3 (6)†	51.6 ± 3.1 (15)§
A_A(ae/lu), %	43.9 ± 1.4 (10)	36.8 ± 0.8 (11)¶	35.4 ± 2.1 (6)§	32.1 ± 1.4 (15)
V(ae), μl	52.2 ± 2.3 (10)	46.1 ± 1.9 (11)*	35.0 ± 3.0 (6)‖	36.9 ± 2.2 (15)§
V(ae)/BW, μl/g	15.1 ± 0.9 (10)	15.1 ± 0.8 (11)	20.8 ± 0.9 (6)‖	16.5 ± 1.1 (15)‡

Definition of abbreviations: A_A(ae/lu), areal density of air-exchanging parenchyma; BW, body weight; V(ae), volume of air-exchanging parenchyma; WT, wild-type.

Values are mean ± SEM of (n) animals examined at P7.

* $P < 0.05$ versus normoxic wild-type animals.

† $P < 0.0001$ versus same-strain normoxic animals.

‡ $P < 0.05$ versus hyperoxic wild-type animals.

§ $P < 0.05$ versus same-strain normoxic animals.

¶ $P < 0.001$ versus normoxic wild-type animals.

‖ $P < 0.005$ versus same-strain normoxic animals.

of the animal being analyzed. Protein levels of the tyrosine kinase flk-1 (VEGF receptor-2) and vascular endothelial growth factor (VEGF) in lung lysates were determined by Western blot analysis using anti–flk-1 and anti-VEGF antibodies (Santa Cruz Biotechnology).

Analysis of Apoptosis-Related Gene Expression

RNase protection assay (RPA) was used to detect and quantify Fas/FasL-related and Bax/Bcl-2-related mRNAs in lung homogenates, as described elsewhere (35). RPA was performed using the RiboQuant RNase Protection Assay kit with the mouse apoptosis-related mAPO-2 and mAPO-3 multi-probe template sets (BD Biosciences, San Diego, CA). The mAPO-2 template set contains DNA templates for bcl-W, bfl1, bcl-$_{XL}$, bcl-XS, bak, bax, bcl2, bad, and the "housekeeping" genes L32 and GAPDH. The mAPO-3 template set contains DNA templates for caspase-8, FasL, Fas, FADD, FAP, FAF, TRAIL, L32, and GAPDH. Band intensities were normalized to that of GAPDH in the same reaction.

Fas and FasL protein levels were evaluated by Western blot analysis of whole lung homogenates using polyclonal anti-Fas (M-20; Santa Cruz Biotechnology, Santa Cruz, CA) and polyclonal anti-FasL (C-178, Santa

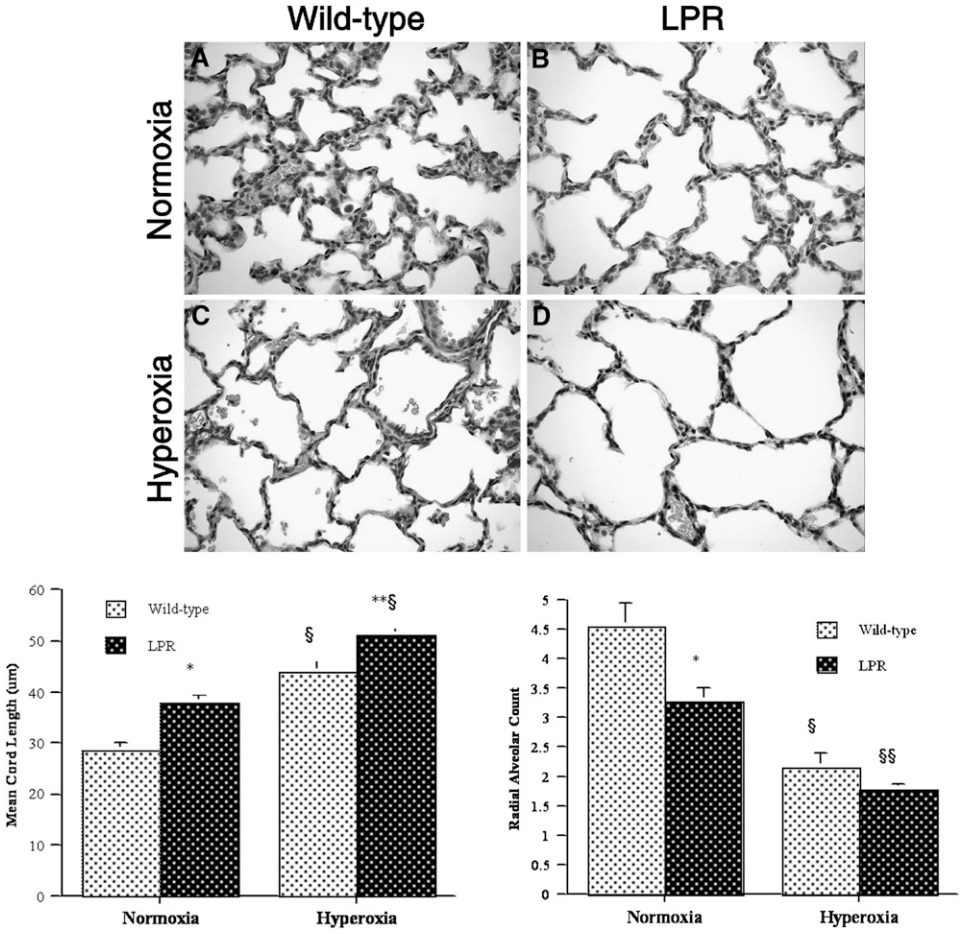

Figure 1. Morphology and morphometry of alveolarization of murine lungs at Postnatal Day (P)7. *Top*: morphology of lpr and wild-type lungs at P7. (*A*) Representative photomicrograph of normoxic wild-type lung showing abundant secondary crests and well-formed alveolar complexes, consistent with mid-alveolarization stage. (*B*) Normoxic *lpr* lung showing larger and less complex airspaces with marked paucity of secondary crests and fully formed alveoli. (*C*) Hyperoxic wild-type lung showing markedly enlarged and simplified airspaces with thin-walled septa; only few secondary crests are present. (*D*) Hyperoxic *lpr* lung showing prominent enlargement and simplification of the airspaces with virtual absence of secondary crests (hematoxylin and eosin staining; *original magnification*: ×400). *Bottom*: mean cord length and radial alveolar count. *Bottom left*: mean cord length. *$P < 0.0002$ versus normoxic wild-type mice; **$P < 0.05$ versus hyperoxic wild-type mice; §$P < 0.001$ versus corresponding normoxic mice. *Bottom right*: radial alveolar count. *$P < 0.02$ versus normoxic wild-type mice; §$P < 0.01$ versus normoxic wild-type mice; §§$P < 0.001$ versus normoxic *lpr* mice.

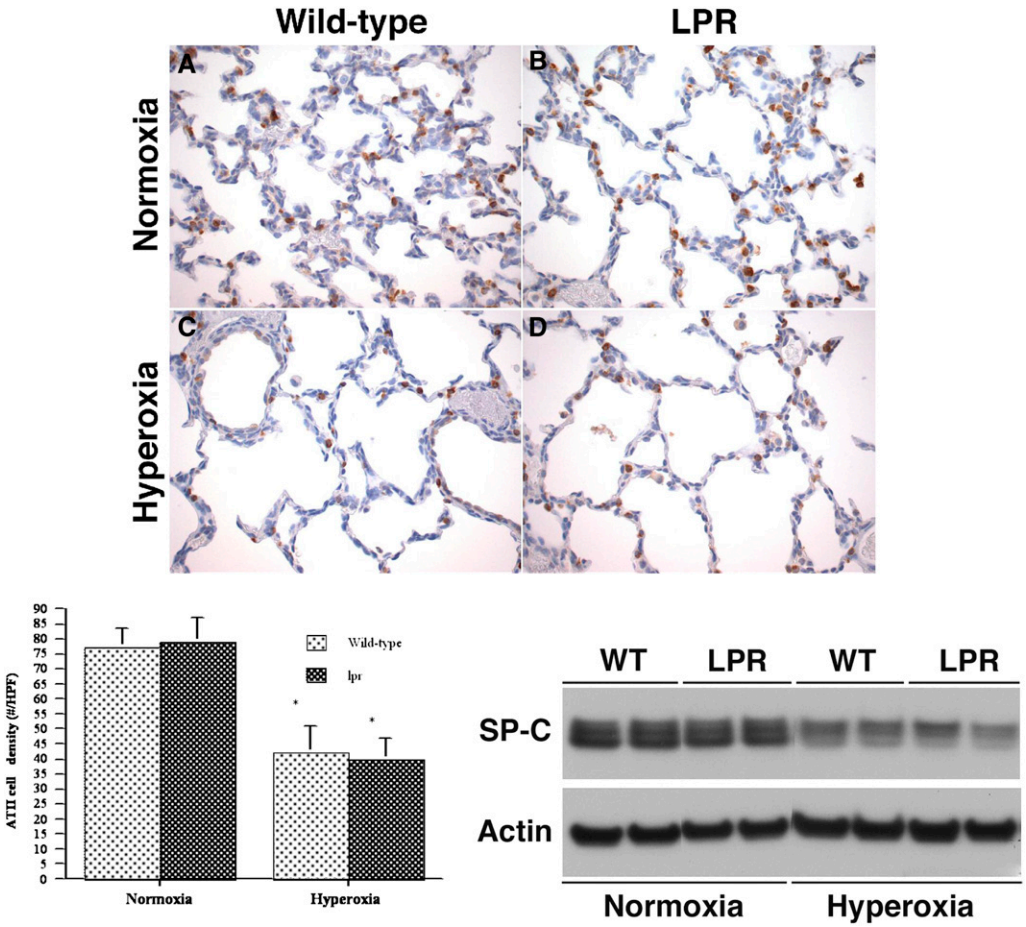

Figure 2. Analysis of surfactant system and microvascular development. *Top*: analysis of surfactant system. (*A–D*) Representative pro–surfactant protein-C (pro–SP-C) immunostaining of lungs of normoxic or hyperoxic wild-type (WT) and *lpr* mice at P7. (*A*) Normoxic wild-type lung. (*B*) Normoxic *lpr* lung. (*C*) Hyperoxic wild-type lung. (*D*) Hyperoxic *lpr* lung. (Anti–SP-C/DAB labeling; hematoxylin counterstain, *original magnification*: ×200). *Bottom left*: Alveolar type II cell density. $*P < 0.02$ versus corresponding normoxic animals. *Bottom right*: Western blot analysis of SP-C protein levels in lung lysates. ***Figure 2 (continued)***: analysis of microvascular development. *Top left*: (*A–D*) Representative Factor VIII (von Willebrand factor) immunostaining of lungs of normoxic or hyperoxic wild-type (WT) and *lpr* mice at P7. (*A*) Normoxic wild-type lung. (*B*) Normoxic *lpr* lung. (*C*) Hyperoxic wild-type lung. (*D*) Hyperoxic *lpr* lung. (anti–Factor VIII/DAB labeling; hematoxylin counterstain, *original magnification*: ×200). *Top right*: Vascular density, expressed as number of vessels (20–80 μm) per ×20 high-power field. Values are mean ± SD of at least four animals studied per group. $*P < 0.05$ versus normoxic wild-type lung; $^{\S}P < 0.005$ versus corresponding normoxic animals. *Bottom left*: Western blot analysis of VEGF and Flk-1 protein levels in lung lysates. *Bottom right*: Densitometry of Flk-1 Western blot analysis. Values are mean ± SD IOD/IOD actin. At least four animals were studied per time point. $*P < 0.05$ versus normoxic wild-type animals; $^{\S}P < 0.02$ versus corresponding hyperoxic animals.

Cruz) antibodies, as described in detail elsewhere (35). Band intensity was expressed as the Integrated Optical Density (IOD) of relevant bands, normalized to the IOD of actin bands (loading control, monoclonal anti-actin; Chemicon International, Temecula, CA). Specificity controls included preincubation of the antibody with blocking peptide.

Analysis of Apoptosis

Pulmonary apoptotic activity was localized and quantified by terminal deoxynucleotidyl transferase-mediated dUTP-FITC nick-end (TUNEL) labeling, as previously described (35, 36). Negative controls for TUNEL labeling omitted the transferase enzyme. For quantification of TUNEL signals, a minimum of 25 high-power fields were viewed per sample, and the number of apoptotic nuclei per high-power field (Apoptotic Index [AI]) was recorded. To estimate the specific rates of alveolar type II cell apoptosis, TUNEL labeling was combined with immunohistochemical detection of alveolar type II cells using an anti–pro–SP-C) antiserum (Abcam Inc., Cambridge, MA), as described (36, 37). Negative controls included omission of the primary antibody, which abolished all labeling.

Processing and cleavage of the key Fas-dependent executioner caspase, caspase-3, was assayed by Western blot analysis of lung homogenates, as described elsewhere (14, 35). Caspase-3 is expressed as an inactive 32-kD precursor from which the 17-kD and 20-kD subunits of the mature caspase-3 are proteolytically generated during apoptosis. The rabbit polyclonal anticaspase-3 antibody used (H-277; Santa Cruz) detects the 32-kD precursor caspase as well as the 17- and 20-kD cleavage products generated during apoptosis. Secondary goat antibody was conjugated with HRP and blots developed with an ECL detection assay (Amersham Pharmacia Biotech, Piscataway, NJ). Specificity controls included preincubation of antibody with blocking peptide.

Analysis of Proliferation

Cell proliferation in *lpr* and wild-type lungs was studied by immunohistochemical detection of the proliferation marker Ki-67 (38). Bound antibody was detected using the ABC immunoperoxidase system with a monoclonal mouse anti-human Ki-67 antibody (BD Biosciences, San Jose, CA), followed by DAB treatment and a light hematoxylin counterstain. The Ki-67 labeling index of air-exchanging parenchyma was determined by manually counting the number of Ki-67–positive nuclei relative to the total number of nuclei (proliferative index) within distal lung parenchyma. For each lung, at least 10 randomly selected fields per slide were evaluated (magnification ×400).

Analysis of ERK1/2 and PI3K/Akt Activation

Activation of ERK1/2 MAP kinase was assayed by Western blot analysis of lung lysates using an antibody to the active phosphorylated kinase: anti–phospho-ERK1/2 (anti–phospho-p44/42 MAP kinase [Thr202/Tyr204]; Cell Signaling Technology, Danvers, MA). Subsequently, the blot was stripped and reprobed with antibody against the nonphosphorylated kinase (anti-p44/42 MAP kinase; Cell Signaling Technology). Activation of the PI3K/Akt pathway was assessed by Western blot analysis using antibodies to phospho-Akt (anti–phospho-Akt [Ser473]) and total Akt (both from Cell Signaling Technology).

Data Analysis

Values are expressed as mean ± SD or, where appropriate, as mean ± SEM. The significance of differences between wild-type and *lpr* mice was determined with the unpaired Student's *t* test or ANOVA with *post hoc* Scheffe-test where indicated. The significance level was set at

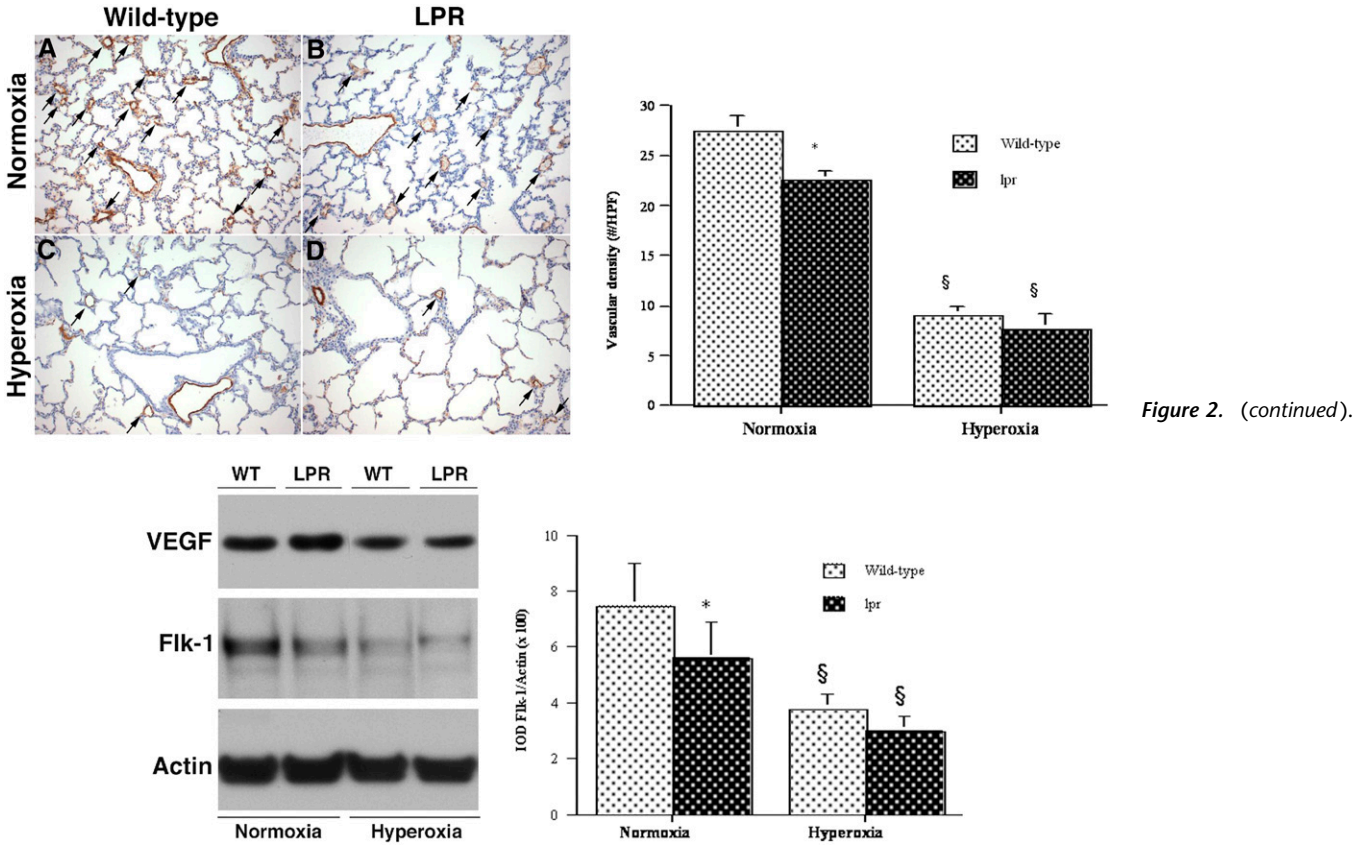

Figure 2. (*continued*).

$P < 0.05$. Statview software (Abacus, Berkeley, CA) was used for all statistical work.

RESULTS

Effects of Hyperoxia on Lung Growth in Newborn *lpr* and Wild-Type Mice

As expected, hyperoxia exposure had an adverse effect on body and lung growth, both in Fas-deficient *lpr* and wild-type mice (Table 1). However, overall survival at P7 was high (> 95%) and similar in wild-type and *lpr* animals. The wet lung weight/body weight ratio was significantly lower in hyperoxia-exposed *lpr* animals compared with hyperoxic wild-type mice (1.77% versus 2.11%, $P < 0.05$). To determine whether the lower lung weight/body weight ratio in hyperoxic *lpr* animals was attributable to decreased lung parenchyma or other factors such as decreased edema fluid, the volume of air-exchanging parenchyma, V(ae), was determined by stereologic volumetry. As shown in Table 1, the V(ae)/body weight ratio was significantly lower in hyperoxic *lpr* mice than in hyperoxic wild-type mice (16.5 μl/g versus 20.8 μl/g), consistent with a relatively smaller lung mass in hyperoxic *lpr* mice.

Analysis of the biometry data in normoxic *lpr* and wild-type mice revealed the lung weight/body weight and V(ae)/body weight ratios to be strikingly similar between both groups (Table 1). In hyperoxic wild-type animals, the lung weight/body weight and V(ae)/body weight ratios exceeded those seen in normoxic wild-type animals, while in hyperoxic *lpr* mice these ratios were similar to those in normoxic *lpr* mice. As the body weights of hyperoxic wild-type and *lpr* mice are similar, these results indicate that hyperoxia induces growth of the lung parenchyma relative to body weight in wild-type mice, while such relative lung expansion appears to be lacking in hyperoxic *lpr* mice.

Effects of Hyperoxia on Alveolarization in Newborn *lpr* and Wild-Type Mice

To determine the potential functional involvement of the Fas/FasL system in hyperoxia-induced alveolar disruption, we compared alveolarization in hyperoxia-exposed wild-type and Fas-deficient *lpr* mice at P7 (mid-alveolarization stage). Lungs of air-exposed wild-type mice at P7 showed thin, well-vascularized alveolar septa with abundant secondary crests and focal alveolar complexes (Figure 1A). Compared with those of wild-type mice, lungs of normoxic *lpr* mice at P7 showed larger and less complex airspaces with focal invaginations of secondary crests but few complete alveoli (Figure 1B). Exposure of newborn wild-type mice to hyperoxia resulted in marked enlargement and simplification of the airspaces, with thinning of the septa and a striking paucity of secondary crests (Figure 1C). Inflammatory cells were inconspicuous. The airspace enlargement of hyperoxia-exposed *lpr* lungs appeared even more prominent than that of wild-type lungs (Figure 1D). The visual impression of impaired alveolarization in hyperoxic *lpr* lungs was confirmed and quantified by morphometric analysis (Figure 1, *bottom*). The MCL of hyperoxic *lpr* lungs was significantly greater than that of wild-type lungs (51.0 ± 1.8 μm in hyperoxic *lpr* lungs versus 43.8 ± 2.4 μm in hyperoxic wild-type lungs, $P < 0.05$), while the radial alveolar count (RAC) tended to be smaller (Figure 1, *bottom*).

In addition to the impairment noted in hyperoxic *lpr* mice, a significant alveolarization defect was identified in normoxic *lpr* mice as well, as evidenced by higher MCL and lower RAC values

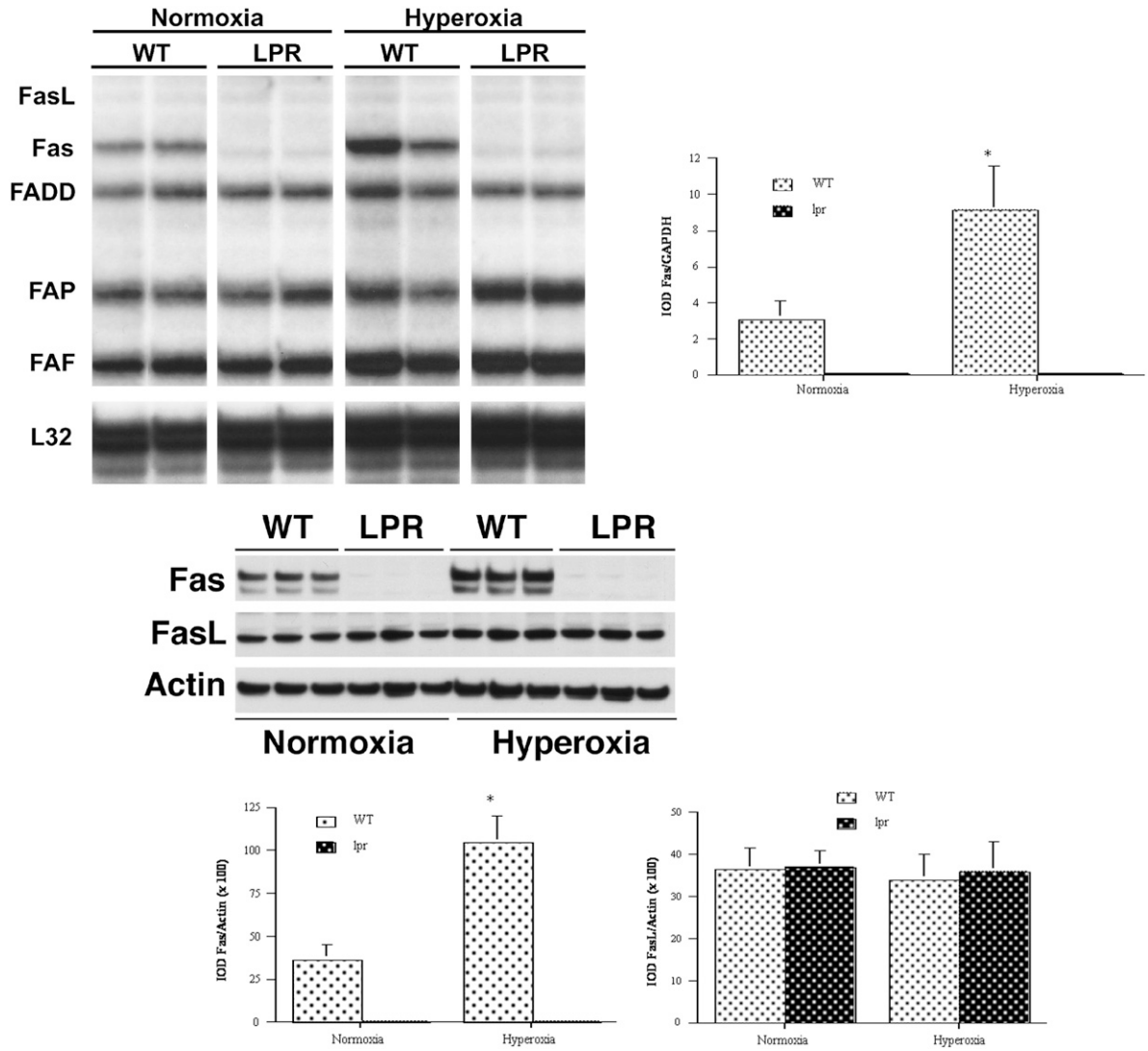

Figure 3. Analysis of Fas-related gene expression. *Top*: RNase protection assay (RPA) of Fas-related mRNA expression in lung lysates. *Left*: RPA assay. *Right*: densitometry of RPA analysis of Fas mRNA. Values are mean ± SD IOD of the gene of interest, normalized to the IOD of constitutively expressed GAPDH mRNA (IOD/IOD GAPDH). Analyses were performed at least in triplicate. *$P < 0.01$ versus corresponding normoxic animals. IOD, integrated optical density; FADD, Fas-associated death domain; FAP, Fas-associated phosphatase-1; FAF, Fas-associated factor-1. The housekeeping genes L32 and GAPDH were included to assess relative RNA loading equality. *Bottom*: Western blot analysis of Fas/FasL protein expression in lung lysates. *Left,* Western blot analysis of Fas and FasL protein expression in lung lysates of mice at P7. Appropriately sized bands were detected for Fas (48 kD) and FasL (40 kD). Actin (42 kD) served as internal loading control. *Right*: densitometry of Fas/FasL Western blot analyses. Values are mean ± SD IOD/IOD actin. At least four animals were studied per time point. *$P < 0.05$ versus corresponding normoxic animals.

compared with age-matched normoxic wild-type mice (Figure 1, *bottom*). To determine whether this alveolarization deficit in newborn *lpr* mice was permanent, we compared the alveolarization parameters in 6-week-old wild-type and *lpr* mice. In these older animals, we did not detect significant differences (not shown), suggesting that alveolarization in normoxic newborn *lpr* mice is delayed, rather than permanently impaired.

Effects of Hyperoxia on the Surfactant System in Newborn *lpr* and Wild-Type Mice

Development of the surfactant system in normoxic and hyperoxic *lpr* and wild-type mice at P7 was assessed by immunohistochemical and Western blot analyses using an anti–pro–SP-C antibody. Exposure to hyperoxia resulted in a 50% reduction of the alveolar type II cell density and a marked decrease in pulmonary SP-C protein levels, both in wild-type and *lpr* mice (Figure 2, *top three panels*). The type II cell density and SP-C protein levels were equivalent in *lpr* and wild-type mice exposed to similar oxygen conditions, suggesting that Fas deficiency did not affect alveolar type II cell cytodifferentiation.

Effects of Hyperoxia on Microvascular Development in Newborn *lpr* and Wild-Type Mice

In view of the intimate relationship between pulmonary microvasculature and alveolar epithelium in postcanalicular lungs, we assessed microvascular development in hyperoxic and normoxic wild-type and *lpr* mice. Growth of the pulmonary microvasculature was quantified by two complementary techniques: morphometric analysis of the density of vascular structures immunoreactive for Factor VIII (vWF) and Western blot analysis of Flk-1 protein levels in lung lysates. In normoxic

conditions, the pulmonary microvascular density and pulmonary Flk-1 levels were significantly lower in *lpr* mice compared with wild-type mice (Figure 2, *continued*), correlating with the deficient alveolarization noted in *lpr* lungs at P7. Exposure to hyperoxia resulted in a dramatic decrease in microvascular density and pulmonary Flk-1 levels, both in *lpr* and wild-type animals. While the vascular density and Flk-1 protein levels tended to be lower in hyperoxic *lpr* mice compared with hyperoxic wild-type mice, this difference did not reach statistical significance. Pulmonary VEGF protein levels were decreased in hyperoxic conditions but similar between *lpr* and wild-type mice within each oxygenation group.

Effects of Hyperoxia on Apoptosis-Related Gene Expression in Newborn Lungs

Steady-state mRNA levels of key Fas/FasL-associated genes in lungs of normoxic and hyperoxic *lpr* and wild-type mice were studied by multitemplate RNase protection assay. Hyperoxia induced a significant 3-fold up-regulation of pulmonary Fas mRNA levels in wild-type mice (Figure 3, *top*). In addition, levels of Fas-associated apoptotic regulators including FADD, FAP, FAF, and RIP were increased to various degrees by hyperoxia exposure. The levels of FAP, FAF, and RIP were equally high in hyperoxic *lpr* and hyperoxic wild-type mice. As expected, Fas mRNA was virtually undetectable in *lpr* mice (Figure 3, *top*). Levels of FasL mRNA were below the detection threshold of this assay in all conditions.

The effects of hyperoxia on pulmonary Fas and FasL protein expression were assessed by Western blot analysis of lung homogenates at P7. As shown in Figure 3 (*bottom*), hyperoxia resulted in a 3-fold increase in pulmonary Fas protein levels in wild-type mice. Hyperoxia had no effect on pulmonary FasL protein levels. Virtually no immunoreactive Fas protein was detected in lungs of *lpr* mice.

To determine the effects of hyperoxia on the expression of the regulators of mitochondrial-dependent apoptosis, the mRNA levels of key Bcl-2/Bax family members were determined by RPA. As shown in Figure 4 and Table 2, hyperoxia induced a significant up-regulation of several apoptotic regulators of the Bax/Bcl-2 family, most notably a 3-fold up-regulation of pro-apoptotic Bax, Bak, and Bad. Levels of anti-apoptotic Bcl-2 were equally low in all conditions studied. The mRNA levels of all mitochondrial-dependent regulators studied were equivalent in wild-type and *lpr* lungs (Figure 4).

Effects of Hyperoxia on Apoptosis in Lungs of Newborn *lpr* and Wild-Type Mice

To begin to determine the mechanisms of differential lung growth in hyperoxic *lpr* versus wild-type mice, we studied their pulmonary apoptotic activity by TUNEL analysis. As shown in Figure 5A, lungs of air-exposed wild-type mice showed relatively few TUNEL-positive nuclei that were scattered within the alveolar septa and in peribronchial and perivascular soft tissue. The apoptotic activity of normoxic *lpr* lungs appeared similar to that of normoxic wild-type lungs (Figure 5B). The pulmonary apoptotic activity of hyperoxia-exposed wild-type mice at P7 was significantly higher than that of normoxic animals (Figure 5C). Abundant TUNEL-positive nuclei were distributed over alveolar epithelial and interstitial compartments. While many nuclei appeared pyknotic or karyorrhectic, as typically seen in cells undergoing apoptotic cell death, other cells showed more diffuse nuclear as well as cytoplasmic TUNEL-reactivity, which may represent an alternative mode of cell death/injury. The TUNEL labeling of hyperoxic *lpr* lungs was equivalent to that of wild-type lungs (Figure 5D).

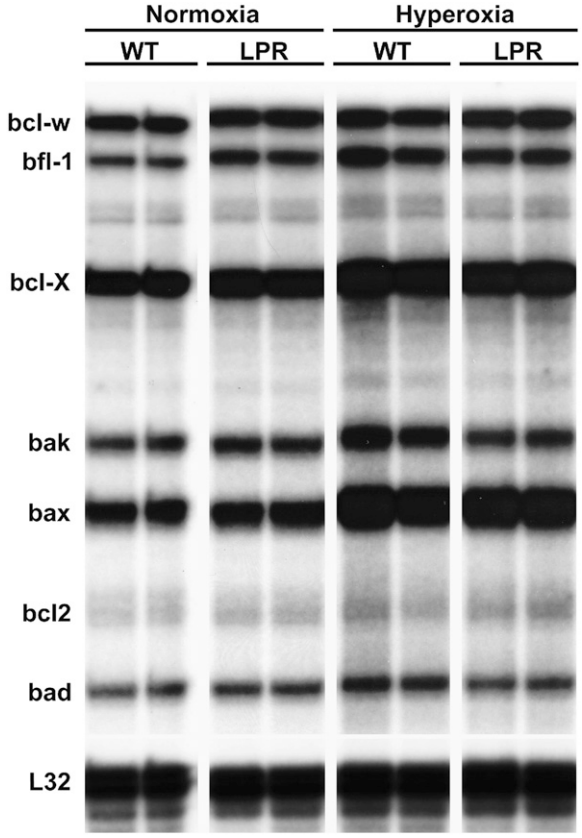

Figure 4. RNase protection assay (RPA) of Bax/Bcl-2-related mRNA expression in lung lysates.

The apoptotic activity of alveolar epithelial type II cells was studied by combining TUNEL labeling with immunohistochemical identification of SP-C–positive type II cells. As shown in Figure 5 (*bottom*), the apoptotic activity of SP-C–positive alveolar type II cells in normoxic conditions was low. Instead, the vast majority of apoptotic cells in normoxic conditions were SP-C–negative interstitial cells, both in wild-type and *lpr* lungs. The apoptotic activity of alveolar type II cells was 3-fold higher in hyperoxic lungs than in normoxic lungs at P7 ($P < 0.05$) (Figure 5, *bottom*). Some TUNEL-positive alveolar type II cells were still attached to the alveolar wall, while others were seen in clusters of SP-C–positive cellular debris within the airspaces

TABLE 2. DENSITOMETRY OF Bcl-2–RELATED RNase PROTECTION ASSAY

	Normoxia		Hyperoxia	
	WT	LPR	WT	LPR
Bax	23.44 ± 2.20	32.92 ± 4.64	62.58 ± 3.51*	64.33 ± 0.91*
Bak	7.33 ± 2.63	12.07 ± 1.05	25.55 ± 4.69*	13.53 ± 2.53†
Bad	4.24 ± 1.78	6.75 ± 0.45	11.31 ± 1.64*	7.41 ± 1.32‡
Bcl-$_{XL/S}$	37.68 ± 0.48	45.30 ± 0.53	56.92 ± 2.78*	57.16 ± 2.91*
Bfl-1	4.61 ± 0.45	11.60 ± 0.95†	18.71 ± 4.61*	15.13 ± 1.37*

Definition of abbreviation: WT, wild-type.

Values represent mean integrated optical density (IOD) of gene of interest normalized to IOD of GAPDH ± SD. At least three animals were studied per group. For Bax, Bak and Bcl-$_{XL/S}$, IOD/IOD GAPDH was multiplied by 100.

* $P < 0.01$ versus normoxia.

† $P < 0.01$ versus corresponding wild-type.

‡ $P < 0.05$ versus corresponding wild-type.

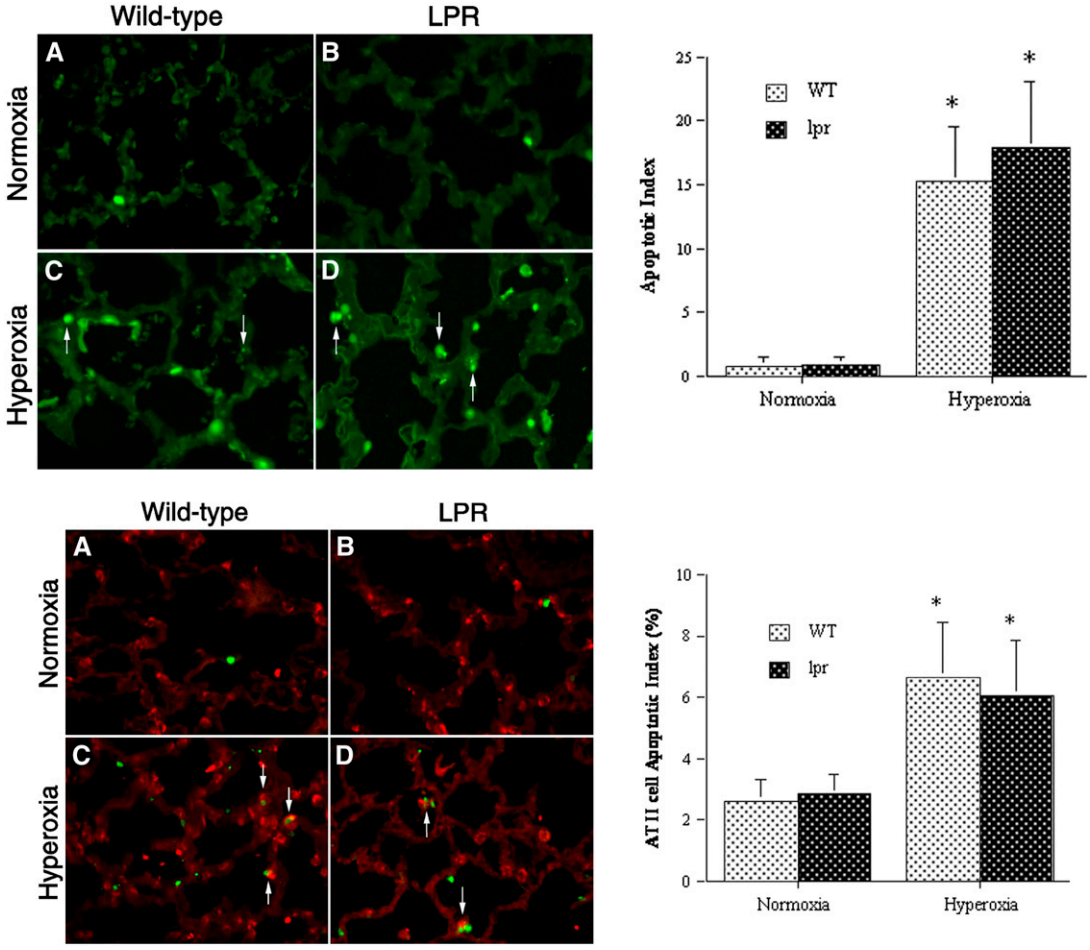

Figure 5. Analysis of apoptosis by TUNEL labeling. *Top*: TUNEL labeling. (*A–D*) Representative TUNEL assays of normoxic and hyperoxic lungs at P7 (*left*). (*A*) Normoxic wild-type lung. (*B*) Normoxic *lpr* lung. (*C*) Hyperoxic wild-type lung. (*D*) Hyperoxic *lpr* lung. Rare TUNEL-positive cells are noted in alveolar septa of normoxic lungs. TUNEL activity is markedly higher in hyperoxic wild-type and *lpr* lungs. Note the presence of TUNEL-positive pyknotic nuclear fragments, characteristic of apoptosis (*arrows*). Omission of transferase enzyme abolished all FITC labeling (not shown). (TUNEL-FITC labeling; *original magnification*: ×400). *Right*: apoptotic index (AI, number of TUNEL-positive nuclei per high power field). Values represent mean AI ± SD. *$P < 0.01$ versus corresponding normoxic animals. *Bottom*: TUNEL labeling combined with anti–SP-C immunohistochemistry. (*A–D*) Murine lungs at P7. (*A*) Normoxic wild-type lung. (*B*) Normoxic *lpr* lung. (*C*) Hyperoxic wild-type lung. (*D*) Hyperoxic *lpr* lung. TUNEL-positive cells in *A* and *B* represent SP-C–negative apoptotic interstitial cells. *Arrows* in *C* and *D* indicate apoptotic SP-C–positive alveolar epithelial type II cells. Omission of transferase enzyme and anti–SP-C antibody abolished all staining (not shown). (TUNEL-FITC labeling and cy-3–labeled anti–SP-C immunofluorescence; *original magnification*: ×400). *Right*: type II cell apoptotic index. Values represent mean AI ± SD of SP-C–positive cells, expressed as a percentage. *$P < 0.01$ versus corresponding normoxic animals.

(Figure 5, *bottom*). The frequency of apoptotic alveolar type II cells in hyperoxic *lpr* lungs was similar to that in hyperoxic wild-type lungs.

As suggested by others (39), the TUNEL assay may not be specific for internucleosomal DNA fragmentation, such as typically seen in apoptosis; some of the TUNEL reactivity may represent random nonapoptotic DNA damage. To confirm the occurrence of true apoptosis, we performed Western blot analysis of cleavage and processing of the main Fas-dependent executioner caspase, caspase-3. Hyperoxia exposure was associated with significant decrease of precursor caspase levels, consistent with apoptosis (Figure 6). Interestingly, caspase-3 cleavage products were readily visualized in lungs exposed to a 4-day period of hyperoxia, but barely visible after 7 days. We speculate that the loss of visible cleaved caspase bands after prolonged hyperoxia may be due to preferential degradation of the smaller-sized 17- and 20-kD bands by secondary necrosis. Similarly, we described caspase-mediated apoptosis as the first morphologically and biochemically recognizable mode of cell death in murine lung epithelial cells exposed to hyperoxia *in vitro*, which was followed by secondary necrosis (14). The intensity of the cleaved caspase bands tended to be higher in hyperoxic *lpr* lungs compared with wild-type lungs; however, the difference in intensity was not statistically significant. These findings demonstrate that hyperoxia-induced pulmonary apoptotic activity is equivalent in Fas-deficient *lpr* mice compared with wild-type mice, and imply that the Fas/FasL system is not critical in the regulation of hyperoxia-induced pulmonary apoptosis.

Effects of Hyperoxia on Proliferation in Lungs of Newborn *lpr* and Wild-Type Mice

To determine whether the observed difference in hyperoxia-induced lung growth between *lpr* and wild-type mice may be due, at least in part, to different proliferation rates, we studied the pulmonary proliferative activity by immunohistochemical analysis using the proliferation marker Ki67. In both hyperoxic and normoxic animals, Ki67-positive nuclei were present within the alveolar epithelial lining as well as stromal interstitial cells and bronchial epithelial cells (Figure 7). The pulmonary Ki67 labeling index was significantly lower in hyperoxic *lpr* animals compared with wild-type animals (Figure 7). The proliferative activity of normoxic lungs was higher than in hyperoxic lungs, and, again, lower in normoxic *lpr* mice compared with wild-type mice (Figure 7).

Effect of Hyperoxia on Activation of Prosurvival Regulators ERK1/2 and PI3K/Akt in Lungs of Newborn *lpr* and Wild-Type Mice

Taken together, our data indicate that hyperoxia induces relatively more lung growth in wild-type mice compared with

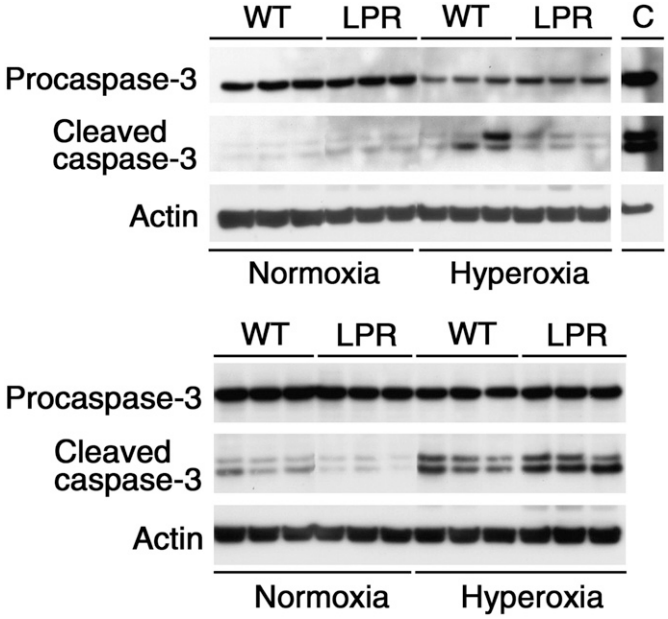

Figure 6. Western blot analysis of caspase-3 cleavage. Analysis of caspase processing in lung lysates of normoxic or hyperoxic wild-type (WT) and *lpr* mice at P7 (*top*) or P4 (*bottom*). Exposure to hyperoxia resulted in cleavage of 32-kD precursor caspase into the 17-kD and 20-kD active subunits. The 17-kD and 20-kD cleavage products were readily visible in hyperoxic lungs at P4. At P7, only some hyperoxic samples revealed faint cleavage bands, despite obviously diminished intensity of the 32-kD precursor caspase bands. Actin served as internal loading control. C: positive control (murine lung epithelial (MLE-12) cells (ATCC no. CRL-2110) exposed to agonistic anti-Fas antibody (clone Jo-2, 20 μg/ml; BD Bioscience).

lpr mice, attributable, in large part, to higher proliferation rates in hyperoxia-exposed wild-type animals. To elucidate the molecular regulation of hyperoxia-induced lung growth and proliferation in wild-type and *lpr* mice, we determined the effects of hyperoxia on expression and activation of two key prosurvival regulators, ERK1/2 and PI3K/Akt. The ERK1/2 and PI3K/Akt cell survival signaling pathways are implicated in the survival of pulmonary epithelial cells after hyperoxic exposure (40–42).

To determine the potential involvement of ERK1/2 in the regulation of hyperoxia-induced Fas-dependent proliferative effects, we studied the effect of hyperoxia exposure on ERK1/2 activation by Western blot analysis of lung lysates. As seen in Figure 8 (*top*), exposure to hyperoxia induced strong stimulation of ERK1/2 tyrosine phosphorylation in wild-type mice without affecting the levels of total ERK1/2. In striking contrast, hyperoxia failed to stimulate ERK1/2 phosphorylation in *lpr* lungs, resulting in dramatically lower pulmonary pERK1/2 levels in hyperoxic *lpr* mice compared with wild-type mice (Figure 8, *top*). In normoxic conditions as well, the levels of the phosphorylated (active) form of ERK1/2 were significantly lower in lungs of *lpr* mice compared with wild-type mice. These experiments suggest the possibility that proliferative signals in hyperoxic newborn lungs are regulated through a Fas/ERK1/2 signaling pathway.

We also analyzed Akt activation in *lpr* and wild-type lungs by Western blotting. Hyperoxia did not have an effect on pulmonary phospo-Akt (pAkt) or total Akt levels (Figure 8, *bottom*). Furthermore, pAkt levels were similar in wild-type and *lpr* lungs, both under normoxic and hyperoxic conditions.

DISCUSSION

In this study, we determined the functional significance of the Fas/FasL pathway in the regulation of hyperoxia-induced apoptosis and alveolar disruption in postcanalicular lungs. To this end, we compared growth kinetics, apoptosis-related gene expression and alveolar development in hyperoxia-exposed newborn wild-type mice with that of age-matched Fas-deficient *lpr* mice bred onto the same genetic background.

Wild-type and Fas-deficient mice were exposed to 95% O_2 from birth to P7. As previously described by others (12), this oxygen regimen resulted in marked enlargement and diminished septation of the airspaces in wild-type mice, replicating the alveolar disruption typical of preterm infants with BPD. In accordance with previous observations in adult and newborn mice (13, 27, 43, 44), hyperoxia induced a dramatic increase in pulmonary apoptosis, involving alveolar type II cells as well as surfactant-negative stromal cells.

Hyperoxia-induced apoptosis was associated with significant 3-fold up-regulation of pulmonary Fas mRNA and protein levels in newborn wild-type mice, in agreement with studies in adult mice (27) and our *in vitro* observations (14). If the Fas/FasL system was a critical regulator of hyperoxia-induced apoptosis and alveolar disruption, we would expect to see less apoptosis and, consequently, a larger mass of lung parenchyma in *lpr* lungs. Paradoxically, however, the lung mass of hyperoxic *lpr* mice was smaller than that of hyperoxic wild-type mice and associated with more profound alveolar disruption. Furthermore, the levels of pulmonary apoptosis were similar in both groups.

Thus, whereas Fas deficiency did not have an impact on hyperoxia-induced pulmonary apoptosis, lung growth and proliferation were significantly diminished in hyperoxic *lpr* mice compared with wild-type mice. The growth deficit in *lpr* mice suggests that the predominant function of the Fas/FasL system in hyperoxic newborn lungs is pro-proliferative, rather than pro-apoptotic. To begin to elucidate the regulation of hyperoxia-induced Fas-dependent proliferation, we studied the expression and activation of extracellular signal–regulated kinases (ERK1/2) in hyperoxic *lpr* and wild-type lungs. ERK1/2 is a member of the MAPkinase family, which comprises three major signaling pathways, each with distinct terminal kinases: ERK1/2, the c-Jun N-terminal kinase (JNK), and the p38 MAP kinase (45). These pathways fulfill fundamental roles in cell growth, cell function, cell differentiation, and cell death. Among the major MAPkinase family members, the ERK1/2 pathway mainly responds to activation by mitogenic stimuli and is generally involved in the regulation of cell proliferation (45), while p38 MAPK and JNK usually promote cell death (46). Activation of the ERK1/2 pathway has been previously reported in lung epithelial cells after hyperoxic exposure. ERK activation in lung epithelial cells has a protective effect in hyperoxia-induced cell death, and prolongs cell survival (40, 42, 47, 48).

To determine the potential functional involvement of ERK1/2 as mediator of hyperoxia-induced, Fas-dependent proliferation, we studied its activation by Western blot analysis of lung homogenates of hyperoxic *lpr* and wild-type mice. We determined that hyperoxia induced significant ERK1/2 activation in wild-type lungs, without affecting levels of total ERK1/2. In contrast, hyperoxia did not lead to ERK1/2 activation in Fas-deficient *lpr* lungs. These findings suggest that ERK1/2 plays a role in the functional coupling of Fas to proliferation in hyperoxic lungs.

In addition to being defective in hyperoxic newborn *lpr* mice, alveolarization and lung growth were also impaired in normoxic *lpr* mice. Impaired alveolarization in newborn *lpr* mice

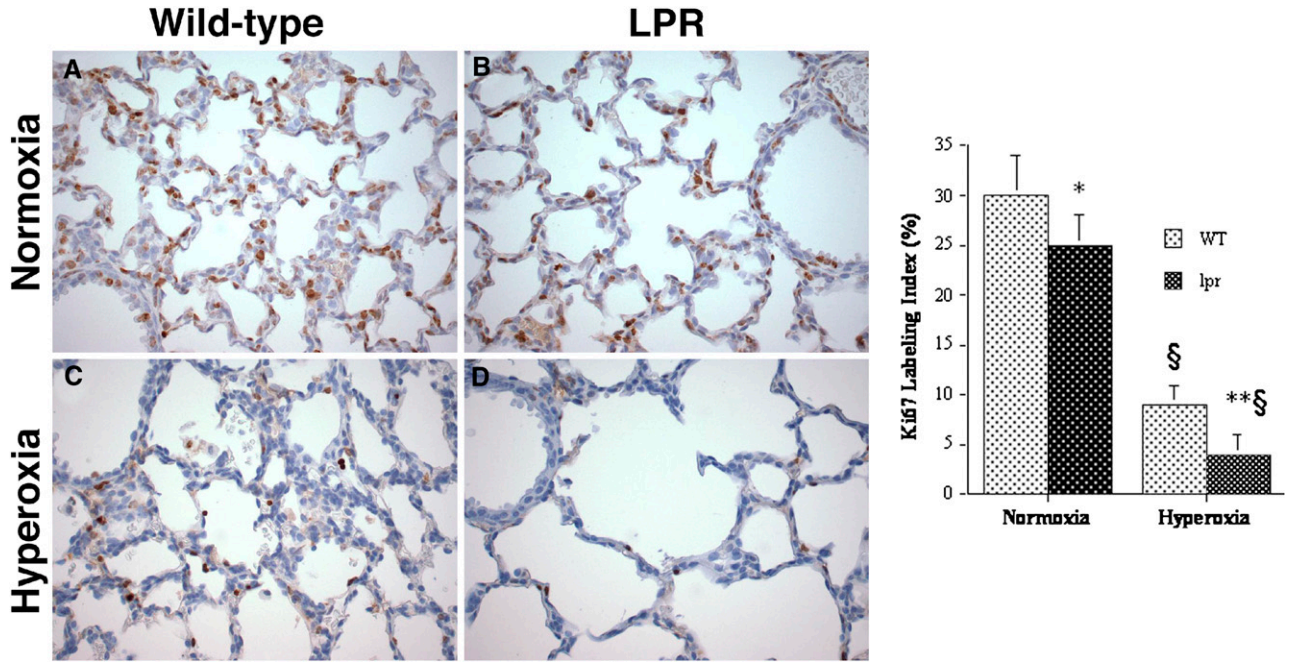

Figure 7. Analysis of proliferation by Ki67 labeling. *Top*: murine lungs at P7. (*A*) Normoxic wild-type lung. (*B*) Normoxic *lpr* lung. (*C*) Hyperoxic wild-type lung. (*D*) Hyperoxic *lpr* lung. Omission of primary antibody abolished all labeling (not shown). (Anti-Ki67/DAB labeling; hematoxylin counterstain, *original magnification*: ×400.) *Right*: Ki67 labeling index (Ki67-LI, number of Ki67-positive nuclei per total number of nuclei, expressed as a percentage). Values represent mean Ki67-LI ± SD. *$P < 0.01$ versus normoxic wild-type mice; **$P < 0.05$ versus hyperoxic wild-type mice; §$P < 0.001$ versus corresponding normoxic mice.

appeared to be developmentally regulated. By 6 weeks of life, the lungs of wild-type and *lpr* mice showed similar MCL and radial alveolar count. Pulmonary growth or maturation defects in Fas- or FasL-deficient mice have not been reported previously. This may be attributed to the fact that the alveolar anomalies of newborn Fas-deficient mice are temporal, compatible with life—at least in nonchallenged conditions—and largely dependent on sensitive morphometric techniques for identification.

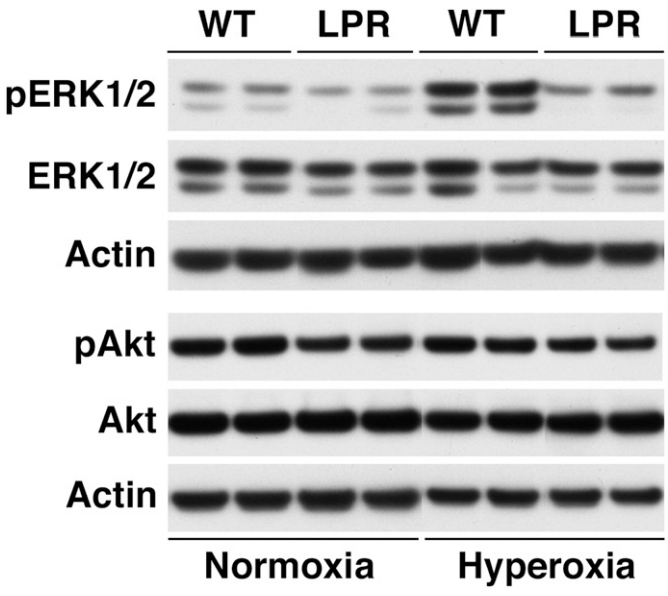

Figure 8. Western blot analysis of pulmonary ERK1/2 and PI3K/Akt activation in lung lysates of mice at P7. Actin (42 kD) served as internal loading control.

Our studies indicate that the Fas system confers proliferation capacity and partial protection against alveolar disruption in hyperoxic newborn lungs. While seemingly paradoxical, this novel proliferative function of Fas/FasL signaling during alveolarization is consistent with an increasing body of evidence suggesting that Fas/FasL signaling has important nonapoptotic functions in addition to its better known apoptotic effects. Fas stimulation can enhance proliferation in lymphocytes, fibroblasts, hepatocytes, cardiomyocytes, and in tumor cells of many different tissue origins (49–58). In addition to promoting proliferation and activation, Fas engagement can also trigger inflammatory changes, including the release of IL-6 and IL-8 (59, 60) and up-regulation of cell surface integrins (61). Finally, Fas engagement has been shown to be capable of inducing angiogenesis (62).

We have previously demonstrated that engagement of the Fas receptor in newborn lungs, either by activating anti-Fas antibody (35) or respiratory epithelium-specific FasL overexpression (63), results in increased alveolar epithelial apoptosis and disrupted alveolar remodeling. The present study implicates the Fas/FasL system as regulator of proliferation in hyperoxic lungs. To integrate the apoptotic and proliferative functions of Fas in postcanalicular lungs, the following unifying paradigm is proposed (Figure 9). Fas activation can trigger either apoptotic or proliferative events. Under normoxic and nonstimulated conditions, both pathways are in equilibrium, although proliferative effects may transiently dominate during the first postnatal week. Fas activation in normoxic conditions, either by agonistic anti-Fas antibody or FasL overexpression, results in activation of the "classical" Fas-dependent apoptotic cascade. This overshadows any Fas-dependent proliferative effects. Hyperoxic conditions increase Fas expression and activate

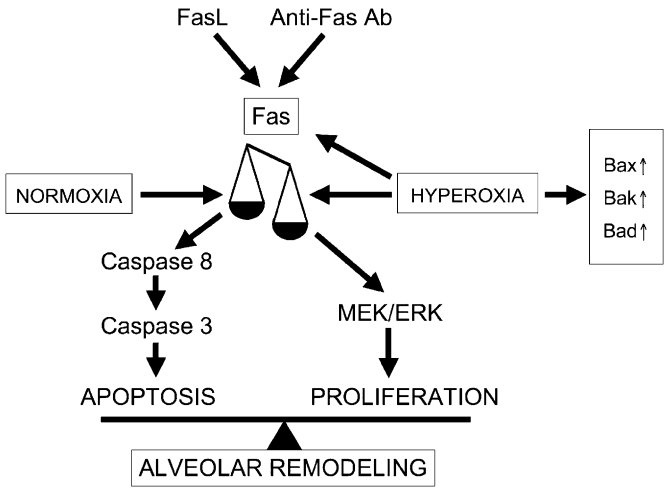

Figure 9. Proposed model for Fas-dependent apoptotic versus proliferative signaling.

a molecular switch, diverting Fas-dependent signaling toward a proliferative pathway that involves activation of the prosurvival MAPkinase, ERK1/2. Hyperoxia-induced Fas-dependent proliferation and growth counteract, in part, the apoptotic effects mediated by hyperoxia-induced Fas-independent apoptotic pathways, resulting in attenuation of alveolar disruption. In the absence of Fas, hyperoxia fails to activate the proliferative Fas-dependent pathway. Consequently, apoptosis by Fas-independent pathways, such as those regulated by the Bax/Bcl-2 family members, is noncompensated, resulting in more profound loss of lung tissue and alveolar disruption.

The putative molecular switch regulating Fas-dependent life-versus-death decisions in hyperoxic newborn lungs remains to be determined. Several possible mechanisms have been implicated in the regulation of the balance of Fas-induced signaling between apoptosis and proliferation, including oxidative stress, ligand dose, caspase 8/FLIP ratio, growth factors, cytokines, and expression/activation of survival pathways such as PI3K/Akt (reviewed in Refs. 64 and 58). To determine the possible role of the PI3K/Akt pathway in the regulation of hyperoxia-induced Fas-dependent proliferation in newborn lungs, we compared the expression/activation status of pulmonary Akt in normoxic and hyperoxic wild-type and *lpr* mice. We determined that hyperoxia had no effect on levels of active pAkt. Furthermore, the pulmonary pAkt levels were similar in *lpr* and wild-type mice, both in normoxic and hyperoxic conditions. These findings suggest that Akt-mediated survival is not critically involved in the regulation of hyperoxia-induced Fas-dependent proliferation/apoptosis decisions in newborn lungs.

The pulmonary apoptotic activity of hyperoxic *lpr* lungs was similar to that of wild-type lungs, suggesting that the Fas/FasL signaling pathway is not essential for activation of hyperoxia-induced apoptosis in newborn lungs. Rather than the Fas/FasL-system, members of the mitochondrial-dependent pathway are likely candidate regulators of hyperoxia-induced apoptosis in newborn lungs. In the present studies, hyperoxia induced significant up-regulation of major pro-apoptotic members of the Bax/Bcl-2 family to the same extent in wild-type and *lpr* mice. Similarly, hyperoxia exposure has been reported to modulate Bcl-2 family members in adult animals (Bax, Bcl-X, Bid) (12, 27, 44, 65, 66). Of note, hyperoxia exposure in adult animals also affects expression of other cell death-related molecules, such as p53 and $p21^{Cip1/WAF1/Sdi1}$ (p21) (27, 65, 67–70). These were not evaluated in this study, but may also be relevant in newborn lungs.

Parenthetically, our *in vivo* results are in apparent contradiction with our previous *in vitro* studies (14). Indeed, whereas the Fas/FasL system was found to be a critical regulator of hyperoxia-induced apoptosis in transformed murine lung epithelial (MLE-12) cells *in vitro*, Fas appears to play no role in hyperoxia-induced lung apoptosis *in vivo*. The mechanism behind the apparent contradiction between the *in vitro* and *in vivo* findings remains to be determined. It is possible, however, that cell-protective mechanisms that are available in intact lungs may not be functional in transformed cells derived from malignant neoplasms. The discrepancy between the *in vitro* and *in vivo* findings illustrates the importance of *in vivo* verification of results obtained in cell culture systems.

In summary, our results suggest that the primary function of the Fas/FasL system in hyperoxic newborn lungs is to signal lung growth and proliferation, thus compensating, in part, for the lung injury and apoptosis caused by non-Fas apoptotic pathways. The Fas-dependent hyperoxia-induced proliferative effects are likely mediated by activation of the prosurvival MAPkinase, ERK1/2. Further studies are required to determine the signaling components that link the Fas receptor to proliferative decisions in postcanalicular lungs.

Conflict of Interest Statement: None of the authors has a financial relationship with a commercial entity that has an interest in the subject of this manuscript.

Acknowledgments: The authors are grateful to Virginia Hovanesian for invaluable technical assistance. They thank James F. Padbury, M.D., for critical review of the manuscript.

References

1. Jobe AH, Ikegami M. Mechanisms initiating lung injury in the preterm. *Early Hum Dev* 1998;53:81–94.
2. Jobe AH, Bancalari E. Bronchopulmonary dysplasia. *Am J Respir Crit Care Med* 2001;163:1723–1729.
3. Palta M, Gabbert D, Weinstein MR, Peters ME. Multivariate assessment of traditional risk factors for chronic lung disease in very low birth weight neonates. The Newborn Lung Project. *J Pediatr* 1991;119:285–292.
4. Husain AN, Siddiqui NH, Stocker JT. Pathology of arrested acinar development in postsurfactant bronchopulmonary dysplasia. *Hum Pathol* 1998;29:710–717.
5. Jobe AJ. The new BPD: an arrest of lung development. *Pediatr Res* 1999;46:641–643.
6. Coalson JJ. Pathology of chronic lung disease in early infancy. In: Chronic lung disease in early infancy. Bland RD, Coalson JJ, editors. New York: M. Dekker; 2000. pp. 85–124.
7. De Paepe ME, Mao Q, Powell J, Rubin SE, DeKoninck P, Appel N, Dixon M, Gundogan F. Growth of pulmonary microvasculature in ventilated preterm infants. *Am J Respir Crit Care Med* 2006;173:204–211.
8. Crapo JD, Barry BE, Foscue HA, Shelburne J. Structural and biochemical changes in rat lungs occurring during exposures to lethal and adaptive doses of oxygen. *Am Rev Respir Dis* 1980;122:123–143.
9. Majno G, Joris I. Apoptosis, oncosis, and necrosis: an overview of cell death. *Am J Pathol* 1995;146:3–15.
10. Mantell LL, Horowitz S, Davis JM, Kazzaz JA. Hyperoxia-induced cell death in the lung–the correlation of apoptosis, necrosis, and inflammation. *Ann N Y Acad Sci* 1999;887:171–180.
11. Mantell LL, Shaffer TH, Horowitz S, Foust R III, Wolfson MR, Cox C, Khullar P, Zakeri Z, Lin L, Kazzaz JA, *et al.* Distinct patterns of apoptosis in the lung during liquid ventilation compared with gas ventilation. *Am J Physiol Lung Cell Mol Physiol* 2002;283:L31–L41.
12. McGrath-Morrow SA, Stahl J. Apoptosis in neonatal murine lung exposed to hyperoxia. *Am J Respir Cell Mol Biol* 2001;25:150–155.
13. Otterbein LE, Chin BY, Mantell LL, Stansberry L, Horowitz S, Choi AM. Pulmonary apoptosis in aged and oxygen-tolerant rats exposed to hyperoxia. *Am J Physiol* 1998;275:L14–L20.
14. De Paepe ME, Mao Q, Chao Y, Powell JL, Rubin LP, Sharma S. Hyperoxia-induced apoptosis and Fas/FasL expression in lung epithelial cells. *Am J Physiol Lung Cell Mol Physiol* 2005;289:L647–L659.
15. Wikenheiser KA, Vorbroker DK, Rice WR, Clark JC, Bachurski CJ, Oie HK, Whitsett JA. Production of immortalized distal respiratory epi-

thelial cell lines from surfactant protein C/simian virus 40 large tumor antigen transgenic mice. *Proc Natl Acad Sci USA* 1993;90:11029–11033.
16. Joza N, Kroemer G, Penninger JM. Genetic analysis of the mammalian cell death machinery. *Trends Genet* 2002;18:142–149.
17. Kroemer G, Reed JC. Mitochondrial control of cell death. *Nat Med* 2000;6:513–519.
18. Nagata S. Fas ligand-induced apoptosis. *Annu Rev Genet* 1999;33:29–55.
19. Sharma K, Wang RX, Zhang LY, Yin DL, Luo XY, Solomon JC, Jiang RF, Markos K, Davidson W, Scott DW, *et al.* Death the Fas way: regulation and pathophysiology of CD95 and its ligand. *Pharmacol Ther* 2000;88:333–347.
20. Walczak H, Krammer PH. The CD95 (APO-1/Fas) and the TRAIL (APO-2L) apoptosis systems. *Exp Cell Res* 2000;256:58–66.
21. Albertine KH, Soulier MF, Wang Z, Ishizaka A, Hashimoto S, Zimmerman GA, Matthay MA, Ware LB. Fas and fas ligand are up-regulated in pulmonary edema fluid and lung tissue of patients with acute lung injury and the acute respiratory distress syndrome. *Am J Pathol* 2002; 161:1783–1796.
22. Hagimoto N, Kuwano K, Nomoto Y, Kunitake R, Hara N. Apoptosis and expression of Fas/Fas ligand mRNA in bleomycin-induced pulmonary fibrosis in mice. *Am J Respir Cell Mol Biol* 1997;16:91–101.
23. Kitamura Y, Hashimoto S, Mizuta N, Kobayashi A, Kooguchi K, Fujiwara I, Nakajima H. Fas/FasL-dependent apoptosis of alveolar cells after lipopolysaccharide-induced lung injury in mice. *Am J Respir Crit Care Med* 2001;163:762–769.
24. Kuwano K, Kawasaki M, Maeyama T, Hagimoto N, Nakamura N, Shirakawa K, Hara N. Soluble form of fas and fas ligand in BAL fluid from patients with pulmonary fibrosis and bronchiolitis obliterans organizing pneumonia. *Chest* 2000;118:451–458.
25. Matute-Bello G, Liles WC, Frevert CW, Nakamura M, Ballman K, Vathanaprida C, Kiener PA, Martin TR. Recombinant human Fas ligand induces alveolar epithelial cell apoptosis and lung injury in rabbits. *Am J Physiol Lung Cell Mol Physiol* 2001;281:L328–L335.
26. Matute-Bello G, Liles WC, Steinberg KP, Kiener PA, Mongovin S, Chi EY, Jonas M, Martin TR. Soluble Fas ligand induces epithelial cell apoptosis in humans with acute lung injury (ARDS). *J Immunol* 1999; 163:2217–2225.
27. Barazzone C, Horowitz S, Donati YR, Rodriguez I, Piguet PF. Oxygen toxicity in mouse lung: pathways to cell death. *Am J Respir Cell Mol Biol* 1998;19:573–581.
28. Tateda K, Deng JC, Moore TA, Newstead MW, Paine R III, Kobayashi N, Yamaguchi K, Standiford TJ. Hyperoxia mediates acute lung injury and increased lethality in murine Legionella pneumonia: the role of apoptosis. *J Immunol* 2003;170:4209–4216.
29. Choo-Wing R, Nedrelow JH, Homer RJ, Elias JA, Bhandari V. Developmental differences in the responses of IL-6 and IL-13 transgenic mice exposed to hyperoxia. *Am J Physiol Lung Cell Mol Physiol* 2007;293:L142–L150.
30. Nagata S, Suda T. Fas and Fas ligand: lpr and gld mutations. *Immunol Today* 1995;16:39–43.
31. Amy RW, Bowes D, Burri PH, Haines J, Thurlbeck WM. Postnatal growth of the mouse lung. *J Anat* 1977;124:131–151.
32. De Paepe ME, Johnson BD, Papadakis K, Luks FI. Lung growth response after tracheal occlusion in fetal rabbits is gestational age-dependent. *Am J Respir Cell Mol Biol* 1999;21:65–76.
33. De Paepe ME, Johnson BD, Papadakis K, Sueishi K, Luks FI. Temporal pattern of accelerated lung growth after tracheal occlusion in the fetal rabbit. *Am J Pathol* 1998;152:179–190.
34. Aherne WA, Dunnill MS. The estimation of whole organ volume. In: Morphometry. Aherne WA, Dunnill MS, editors. London: Edward Arnold Ltd.; 1982. pp. 10–18.
35. De Paepe ME, Mao Q, Embree-Ku M, Rubin LP, Luks FI. Fas/FasL-mediated apoptosis in perinatal murine lungs. *Am J Physiol Lung Cell Mol Physiol* 2004;287:L730–L742.
36. De Paepe ME, Rubin LP, Jude C, Lesieur-Brooks AM, Mills DR, Luks FI. Fas ligand expression coincides with alveolar cell apoptosis in late-gestation fetal lung development. *Am J Physiol Lung Cell Mol Physiol* 2000;279:L967–L976.
37. De Paepe ME, Sardesai MP, Johnson BD, Lesieur-Brooks AM, Papadakis K, Luks FI. The role of apoptosis in normal and accelerated lung development in fetal rabbits. *J Pediatr Surg* 1999;34:863–870. (discussion 870–861).
38. Scholzen T, Gerdes J. The Ki-67 protein: from the known and the unknown. *J Cell Physiol* 2000;182:311–322.
39. Gold R, Schmied M, Giegerich G, Breitschopf H, Hartung HP, Toyka KV, Lassmann H. Differentiation between cellular apoptosis and necrosis by the combined use of *in situ* tailing and nick translation techniques. *Lab Invest* 1994;71:219–225.
40. Buckley S, Driscoll B, Barsky L, Weinberg K, Anderson K, Warburton D. ERK activation protects against DNA damage and apoptosis in hyperoxic rat AEC2. *Am J Physiol* 1999;277:L159–L166.
41. Lu Y, Parkyn L, Otterbein LE, Kureishi Y, Walsh K, Ray A, Ray P. Activated Akt protects the lung from oxidant-induced injury and delays death of mice. *J Exp Med* 2001;193:545–549.
42. Truong SV, Monick MM, Yarovinsky TO, Powers LS, Nyunoya T, Hunninghake GW. Extracellular signal-regulated kinase activation delays hyperoxia-induced epithelial cell death in conditions of Akt downregulation. *Am J Respir Cell Mol Biol* 2004;31:611–618.
43. Mantell LL, Kazzaz JA, Xu J, Palaia TA, Piedboeuf B, Hall S, Rhodes GC, Niu G, Fein AF, Horowitz S. Unscheduled apoptosis during acute inflammatory lung injury. *Cell Death Differ* 1997;4:600–607.
44. Wang X, Ryter SW, Dai C, Tang ZL, Watkins SC, Yin XM, Song R, Choi AM. Necrotic cell death in response to oxidant stress involves the activation of the apoptogenic caspase-8/bid pathway. *J Biol Chem* 2003;278:29184–29191.
45. Johnson GL, Lapadat R. Mitogen-activated protein kinase pathways mediated by ERK, JNK, and p38 protein kinases. *Science* 2002;298: 1911–1912.
46. Xia Z, Dickens M, Raingeaud J, Davis RJ, Greenberg ME. Opposing effects of ERK and JNK-p38 MAP kinases on apoptosis. *Science* 1995;270:1326–1331.
47. Romashko J III, Horowitz S, Franek WR, Palaia T, Miller EJ, Lin A, Birrer MJ, Scott W, Mantell LL. MAPK pathways mediate hyperoxia-induced oncotic cell death in lung epithelial cells. *Free Radic Biol Med* 2003;35:978–993.
48. Xu D, Guthrie JR, Mabry S, Sack TM, Truog WE. Mitochondrial aldehyde dehydrogenase attenuates hyperoxia-induced cell death through activation of ERK/MAPK and PI3K-Akt pathways in lung epithelial cells. *Am J Physiol Lung Cell Mol Physiol* 2006;291:L966–L975.
49. Alderson MR, Armitage RJ, Maraskovsky E, Tough TW, Roux E, Schooley K, Ramsdell F, Lynch DH. Fas transduces activation signals in normal human T lymphocytes. *J Exp Med* 1993;178:2231–2235.
50. Desbarats J, Newell MK. Fas engagement accelerates liver regeneration after partial hepatectomy. *Nat Med* 2000;6:920–923.
51. Freiberg RA, Spencer DM, Choate KA, Duh HJ, Schreiber SL, Crabtree GR, Khavari PA. Fas signal transduction triggers either proliferation or apoptosis in human fibroblasts. *J Invest Dermatol* 1997;108:215–219.
52. Nelson DP, Setser E, Hall DG, Schwartz SM, Hewitt T, Klevitsky R, Osinska H, Bellgrau D, Duke RC, Robbins J. Proinflammatory consequences of transgenic fas ligand expression in the heart. *J Clin Invest* 2000;105:1199–1208.
53. Alderson MR, Tough TW, Braddy S, Davis-Smith T, Roux E, Schooley K, Miller RE, Lynch DH. Regulation of apoptosis and T cell activation by Fas-specific mAb. *Int Immunol* 1994;6:1799–1806.
54. Shinohara H, Yagita H, Ikawa Y, Oyaizu N. Fas drives cell cycle progression in glioma cells via extracellular signal-regulated kinase activation. *Cancer Res* 2000;60:1766–1772.
55. Borset M, Hjorth-Hansen H, Johnsen AC, Seidel C, Waage A, Espevik T, Sundan A. Apoptosis, proliferation and NF-kappaB activation induced by agonistic Fas antibodies in the human myeloma cell line OH-2: amplification of Fas-mediated apoptosis by tumor necrosis factor. *Eur J Haematol* 1999;63:345–353.
56. Wajant H. The Fas signaling pathway: more than a paradigm. *Science* 2002;296:1635–1636.
57. Siegel RM, Chan FK, Chun HJ, Lenardo MJ. The multifaceted role of Fas signaling in immune cell homeostasis and autoimmunity. *Nat Immunol* 2000;1:469–474.
58. Peter ME, Budd RC, Desbarats J, Hedrick SM, Hueber AO, Newell MK, Owen LB, Pope RM, Tschopp J, Wajant H, *et al.* The CD95 receptor: apoptosis revisited. *Cell* 2007;129:447–450.
59. Choi C, Gillespie GY, Van Wagoner NJ, Benveniste EN. Fas engagement increases expression of interleukin-6 in human glioma cells. *J Neurooncol* 2002;56:13–19.
60. Schaub FJ, Han DK, Liles WC, Adams LD, Coats SA, Ramachandran RK, Seifert RA, Schwartz SM, Bowen-Pope DF. Fas/FADD-mediated activation of a specific program of inflammatory gene expression in vascular smooth muscle cells. *Nat Med* 2000;6:790–796.
61. Jarad G, Wang B, Khan S, DeVore J, Miao H, Wu K, Nishimura SL, Wible BA, Konieczkowski M, Sedor JR, *et al.* Fas activation induces renal tubular epithelial cell beta 8 integrin expression and function in the absence of apoptosis. *J Biol Chem* 2002;277:47826–47833.

62. Biancone L, Martino AD, Orlandi V, Conaldi PG, Toniolo A, Camussi G. Development of inflammatory angiogenesis by local stimulation of Fas in vivo. *J Exp Med* 1997;186:147–152.
63. De Paepe ME, Gundavarapu S, Tantravahi U, Pepperell JR, Haley SA, Luks FI, Mao Q. Fas-ligand-induced apoptosis of respiratory epithelial cells causes disruption of postcanalicular alveolar development. *Am J Pathol* 2008;173:42–56.
64. Lambert C, Landau AM, Desbarats J. Fas-beyond death: a regenerative role for Fas in the nervous system. *Apoptosis* 2003;8:551–562.
65. O'Reilly MA, Staversky RJ, Huyck HL, Watkins RH, LoMonaco MB, D'Angio CT, Baggs RB, Maniscalco WM, Pryhuber GS. Bcl-2 family gene expression during severe hyperoxia induced lung injury. *Lab Invest* 2000;80:1845–1854.
66. Ward NS, Waxman AB, Homer RJ, Mantell LL, Einarsson O, Du Y, Elias JA. Interleukin-6-induced protection in hyperoxic acute lung injury. *Am J Respir Cell Mol Biol* 2000;22:535–542.
67. McGrath SA. Induction of p21WAF/CIP1 during hyperoxia. *Am J Respir Cell Mol Biol* 1998;18:179–187.
68. O'Reilly MA, Staversky RJ, Stripp BR, Finkelstein JN. Exposure to hyperoxia induces p53 expression in mouse lung epithelium. *Am J Respir Cell Mol Biol* 1998;18:43–50.
69. O'Reilly MA, Staversky RJ, Watkins RH, Maniscalco WM. Accumulation of p21(Cip1/WAF1) during hyperoxic lung injury in mice. *Am J Respir Cell Mol Biol* 1998;19:777–785.
70. McGrath-Morrow SA, Cho C, Soutiere S, Mitzner W, Tuder R. The effect of neonatal hyperoxia on the lung of p21Waf1/Cip1/Sdi1-deficient mice. *Am J Respir Cell Mol Biol* 2004;30:635–640.